TECHNICAL REPORT 75-1

FAULTS ON SKYLAB IMAGERY OF THE SALTON TROUGH AREA, SOUTHERN CALIFORNIA

June 1975

by

P. M. Merifield and D. L. Lamar
California Earth Science Corporation
1318 Second Street, Suite 27
Santa Monica, California 90401
Telephone: (213) 395-4528

for

David Amsbury, Technical Monitor
NASA Lyndon B. Johnson Space Center
Houston, Texas

Sponsored by NASA Lyndon B. Johnson Space Center
Contract NAS 2-7698

TECHNICAL REPORT 75-1

FAULTS ON SKYLAB IMAGERY OF THE SALTON TROUGH AREA, SOUTHERN CALIFORNIA

June 1975

by

P. M. Merifield and D. L. Lamar
California Earth Science Corporation
1318 Second Street, Suite 27
Santa Monica, California 90401
Telephone: (213) 395-4528

for

David Amsbury, Technical Monitor
NASA Lyndon B. Johnson Space Center
Houston, Texas

Sponsored by NASA Lyndon B. Johnson Space Center
Contract NAS 2-7698

PREFACE

The regional geologic structure displayed on Skylab photos of the Salton Trough area was studied as a part of a broader investigation to apply Skylab images to the analysis of fault tectonics and earthquake hazards of southern California. This research was sponsored by the NASA Lyndon B. Johnson Space Center. A portion of this report was presented at the NASA Earth Resources Survey Symposium, June 8-13, 1975, Houston, Texas and is in press in the Proceedings Volume.

ABSTRACT

Large segments of the major high-angle faults in the Salton Trough area are readily identifiable in Skylab images. Along active faults, distinctive topographic features such as scarps and offset drainage, and vegetation differences due to ground water blockage in alluvium are visible. Other fault-controlled features along inactive as well as active faults visible in Skylab photography include straight mountain fronts, linear valleys and lithologic differences producing contrasting tone, color or texture. A northwestern extension of a fault in the San Andreas set, inferred by recent geophysical work in northwest Sonora, is postulated by the regional alignment of possible fault-controlled features. The suspected fault is covered by Holocene deposits, principally windblown sand; subsurface exploration would be necessary to verify its existence. A northwest trending tonal change in cultivated fields across Mexicali Valley is visible on Skylab photos. Surface evidence for faulting has not been observed; however, the linear may be caused by differences in soil conditions along an extension of a segment of the San Jacinto fault zone. No evidence of faulting could be found along linears which appear as possible extensions of the Substation and Victory Pass faults, demonstrating that the interpretation of linears as faults in small-scale photography must be corroborated by field investigations. The principal advantage of Skylab images for regional fault studies is the synoptic view which makes regional alignments of structural features apparent. The high resolution is an additional advantage because distinctive fault-controlled topographic features can be identified.

INTRODUCTION

The structure of the Salton Trough is of considerable interest because of the region's geothermal resources and the controversy concerning southeastern extensions of the San Andreas fault zone beyond the southeast end of the Salton Sea. This paper describes the application of Skylab imagery, in conjunction with larger scale photography and field investigations, to improved knowledge of the location and history of movement of faults in the Salton Trough area. The Salton Trough extends from the upper Coachella Valley north of the Salton Sea to the Gulf of California; the regional structure is dominated by the northwest trending San Andreas and San Jacinto fault zones (Fig. 1).

Photos of the Salton Trough taken from Skylab provide a remarkable overview which aids in the interpretation of the regional relationship between structural features. A photo interpretation of faults and linears appearing on Skylab images of the region between the north end of the Salton Trough and the Gulf of California was accomplished. Features identified in this study, and the areas covered by the Skylab images utilized, are shown in Fig. 2, and the individual Skylab images are reproduced as Figs. 3, 4, and 5. Detailed investigations consisting of field studies and aircraft overflights of critical locations were concentrated in the area north of the Salton Sea covered by Figs. 3 and 5. South of the Salton Sea, reconnaissance studies were made of linears which may represent previously unrecognized fault segments along the trends of the San Andreas and San Jacinto fault zones.

SAN ANDREAS FAULT

The San Andreas fault, the major tectonic feature of California, extends for nearly 1000 kilometers (600 miles) southeasterly from the Pacific Ocean near Point Arena to at least a point approximately midway along the eastern shore of the Salton Sea (Fig. 1). The fault is the most recent surface rupture within a zone of roughly parallel fractures that branch and interlace within a zone as much as 10 kilometers (6 miles) wide (Crowell, 1962). The group of major faults roughly parallel to the San Andreas fault in southern

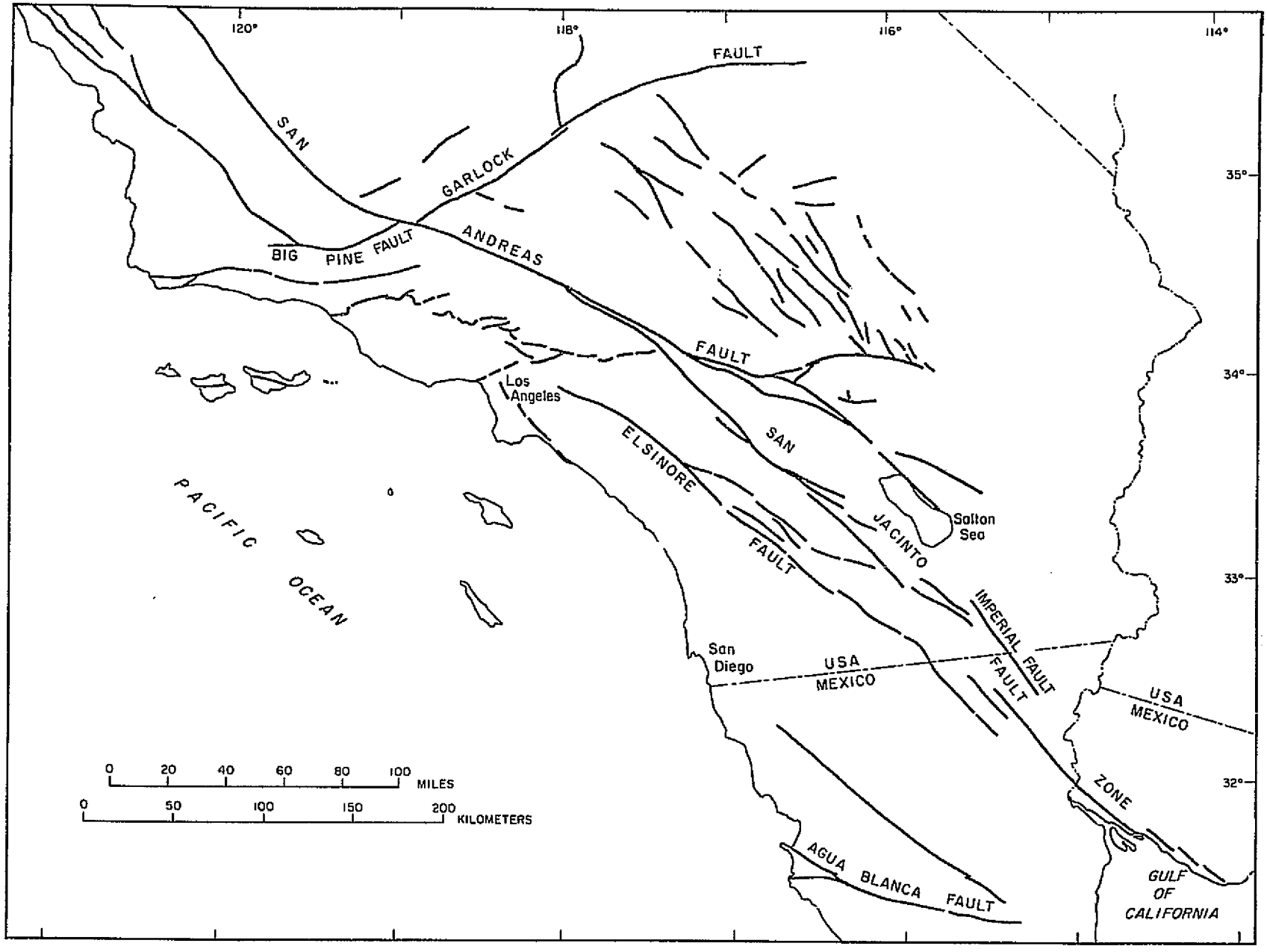

Fig. 1 - Map showing major faults in southern California and northern Mexico. Redrawn from Proctor (1973).

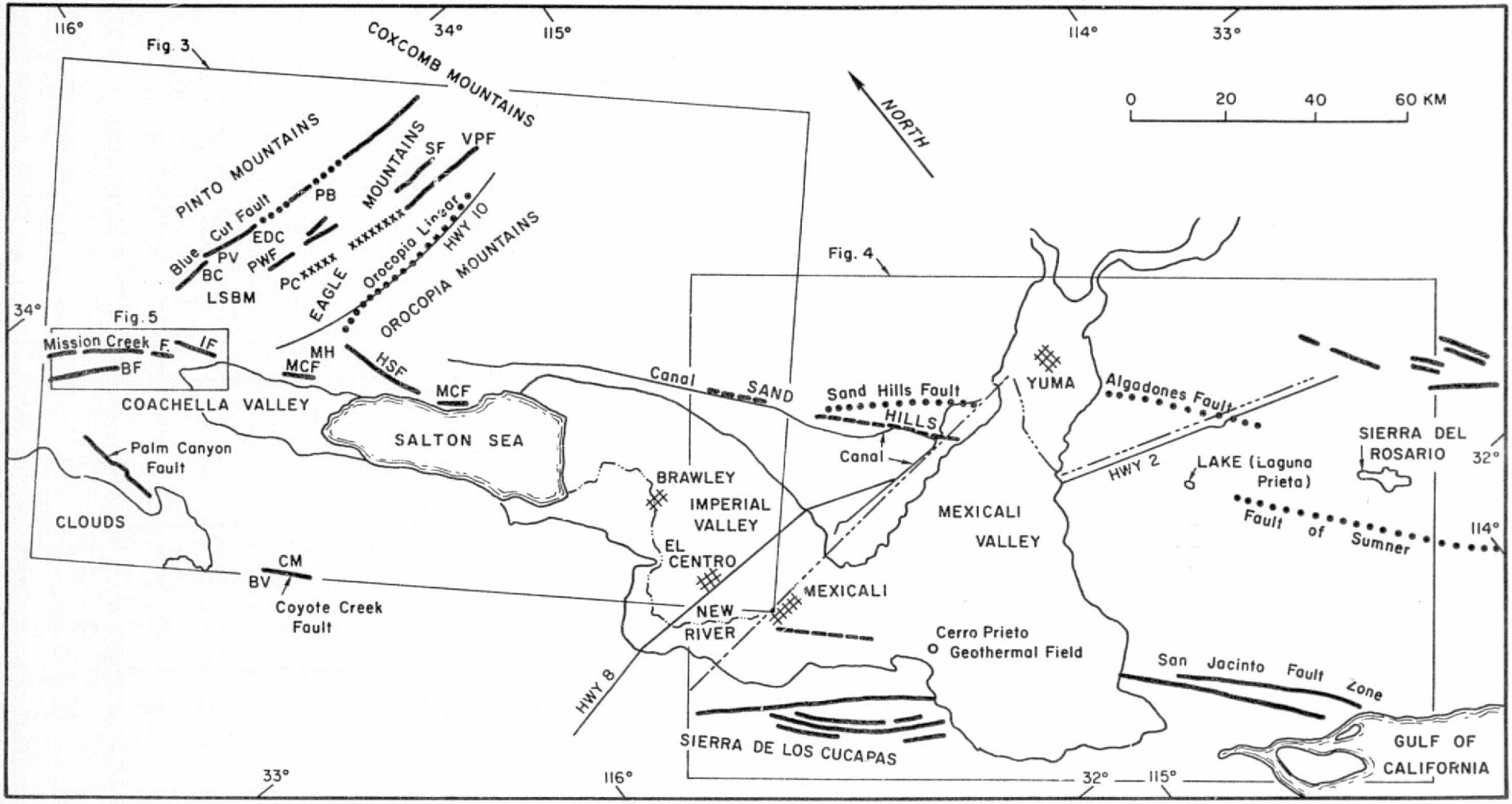

Fig. 2 - Map of Salton Trough and vicinity showing faults and linears seen on Skylab images or discussed in text. The outlines of Skylab images included in this report are indicated. Explanation: solid line: photo linear coincident with known fault or fault line scarp; dashed line: photo linear related to possible surface expression of fault; dotted line: covered fault; xxx: photo linear with no evidence of faulting. Abbreviations: BC: Blue Cut; BF: Banning fault; BV: Borrego Valley; CM: Coyote Mountain; EDC: El Dorado Canyon; HSF: Hidden Springs fault; IF: Indio fault; LSBM: Little San Bernardino Mountains; MCF: Mission Creek fault; MH: Mecca Hills; PB: Pinto Basin; PC: Pinkham Canyon; PV: Pleasant Valley, PWF: Porcupine Wash fault; SF: Substation fault; VPF: Victory Pass fault.

Fig.3 - Salton Sea and vicinity. Portion of Skylab 4, 190A camera, Roll 76, Frame 82 (original in natural color). See Fig. 2 for features identified.

Fig.4 - Salton Trough between Gulf of California and Imperial Valley. Portion of Skylab 2, 190A camera, Roll 4 Frame 134 (original in natural color). See Fig. 2 for features identified.

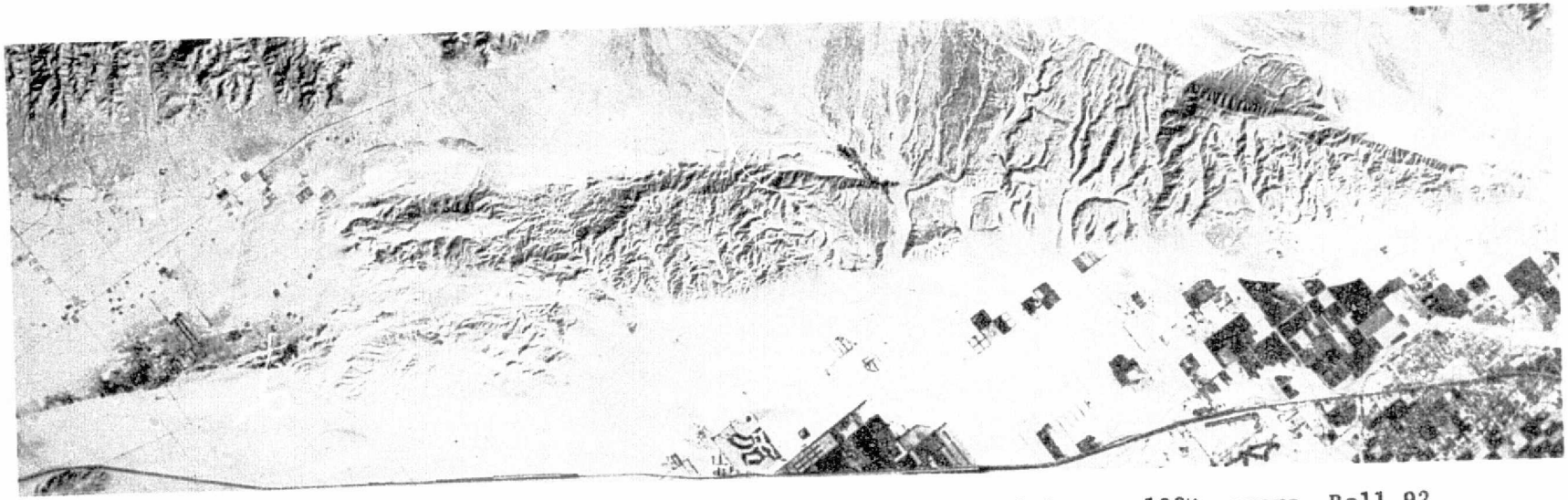

Fig.5 - Indio Hills and vicinity. Enlarged portion of Skylab 4 image, 190B camera, Roll 92, Frame 352 (original in natural color) See Fig.6 for features identified.

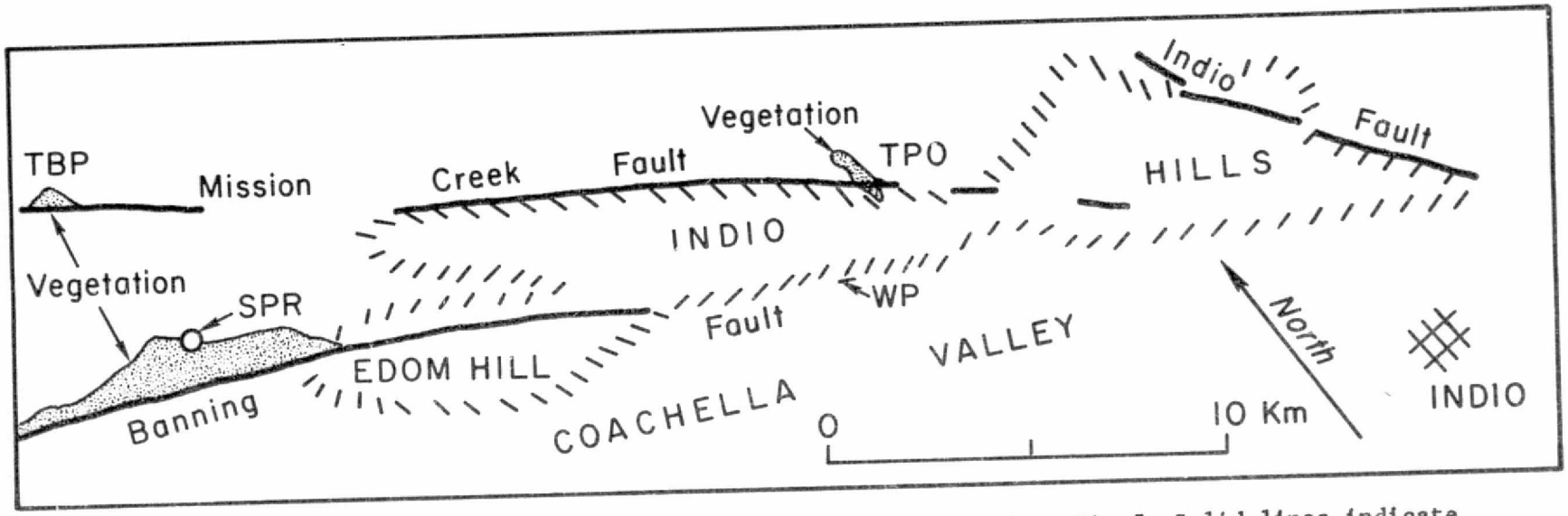

Fig.6 - Map of Indio Hills and vicinity showing features identified on Fig.5. Solid lines indicate prominent linear features along faults discussed in text. Hachured lines indicate boundaries of physiographic features. Abbreviations: SPR: Seven Palms Ranch; TBP: Two Bunch Palms; TPO: Thousand Palms Oasis; WP: Willis Palms.

California, such as the San Jacinto and Elsinore, are included in the San Andreas fault system by Crowell (1962) and Dibblee (1968) and in the San Andreas set by Hill (1965).

Southeast of the Salton Sea, surface evidence of faulting in late Quaternary sediments and seismic activity are lacking; and on the basis of subsurface investigations, Biehler et al (1964) conclude that a southeastern extension of the San Andreas fault cannot be justified. Allen et al (1972) have suggested that the San Andreas fault is a right-lateral transform fault and that activity at the southeast end may terminate at a spreading center. The spreading center could lie between the San Andreas and San Jacinto faults beneath Quaternary volcanic rocks and geothermal anomalies on the southeast shore of the Salton Sea (Elders et al, 1972). According to this hypothesis, northwest trending faults southeast of the termination of the active San Andreas fault would have little or no horizontal displacement but would bring crusts of different age and character into juxtaposition. The eastern edge of the Salton Trough sedimentary basin is possibly delineated by such faults, with abrupt differences in depth to basement. The active San Andreas fault zone in Coachella Valley northwest of the hypothetical spreading center and other known and inferred faults with the same trend to the southeast are described below.

Coachella Valley Area

At the northwest end of Coachella Valley, the Banning and Mission Creek faults comprise the main branches of the San Andreas (Figs. 2 and 6). East of its juncture with the south branch of the San Andreas in San Gorgonio Pass, on the south slope of the San Bernardino Mountains, the Banning fault is a north-dipping thrust fault with basement rocks thrust over Tertiary sediments and Pleistocene gravels (Allen, 1957). To the southeast in Coachella Valley, the Banning fault becomes a "high-angle fault characteristic of the San Andreas with right-slip movements that involve Pleistocene and Recent alluvial sediments" (Dibblee, 1968).

The Mission Creek fault dips steeply (62°-90°) to the northeast. Recent movement is indicated by trenches and scarplets in alluvium, offset streams and dammed ground water, which is hot and shallow on the northeast side of the fault and cold and deep on the southwest side (Proctor, 1958). The

Cabazon Fanglomerate (Holocene) shows a minimum of 330 meters (1100 feet) of vertical separation (north side up), and right-lateral stream offsets up to 240 meters (800 feet) are present in the Indio Hills. Proctor (1958) has suggested that the 1948 Desert Hot Springs earthquake occurred on the Mission Creek fault, but Wallace (1970) has questioned this interpretation.

The Banning fault and Mission Creek fault join directly north of Indio (Fig. 6); from this point the San Andreas fault zone trends about S45°E to the possible spreading center southeast of the Salton Sea. A zone of tightly folded and sheared Cenozoic sediments that form spectacular linear valleys occurs along this portion of the fault (Allen et al, 1972). Displacements up to 1.3 centimeters (.5 inch) and creep along the San Andreas from the Mecca Hills to its terminus east of the Salton Sea were apparently triggered by the 1968 Borrego Mountain earthquake (Allen et al, 1972). These breaks coincide with recently active segments of the San Andreas fault zone mapped by Hope (1969a).

Fig. 5 is an enlarged portion of a Skylab image of the north end of Coachella Valley which shows strands of the San Andreas fault zone and other faults in greater detail. The locations of individual features on Fig. 5 are shown on the sketch map (Fig. 6). Unless otherwise indicated, the faults are most distinct in the aerial color photography; of the black and white bands, the red (.6-.7 μm) is superior for topographic detail, and vegetated areas are most apparent in the color IR.

The Banning fault is visible on Skylab imagery for most of the interval from its convergence with the Mission Creek fault directly north of Indio, to the north end of Coachella Valley. The fault is most prominently delineated as an abrupt break in vegetation for 8 kilometers (5 miles) across the desert surface directly northwest of the Indio Hills (Fig. 7). This is one of the best examples of surface evidence of a buried fault. Thick vegetation, consisting mostly of mesquite but also large trees, is only present on the northeast side of the fault. Southwest of the fault, the desert surface consists mostly of light-colored medium to coarse-grained sand with occasional pebbles. Brown sage bushes are spaced 3-6 meters (10-20 feet) apart. More vegetation is present on the north side of the fault because the fault acts as a barrier to ground water flowing from the north. Northeast of the fault, static water

Fig.7 - Low-altitude aerial view looking northwestward along Banning Fault. San Bernardino Mountains in background.

Fig.8 - Low-altitude aerial view looking eastward along Blue Cut Fault. El Dorado Canyon is in the middle view and Pinto Basin is in the background.

levels are at depths averaging about 10 meters (30 feet); south of the fault the water level is around 100 meters (300 feet) below the surface (Tyley, 1971). Artesian springs are present north of the fault at Seven Palms Ranch.

To the southeast between Edom Hill and the Indio Hills, the trace of the Banning fault is marked by faint differences in tone and a prominent linear valley. The trace along the southwest edge of the Indio Hills is evidenced by the tonal contrast between the desert surface, described above, on the southwest and tan colored Ocotillo Conglomerates of Quaternary age uplifted along the northeast side of the fault. The southwest edge of the Indio Hills is relatively straight, however, no direct physiographic evidence of faulting can be seen on Skylab images of this area. Willis Palms, an oasis along the southwest edge of the Indio Hills, is visible in the Skylab images as a small dark area of vegetation. This is another locality of near-surface ground water caused by subsurface blockage of ground water flow by the Banning fault.

The Mission Creek fault can be traced on the enlarged Skylab image (Fig. 5) over most of its length from Two Bunch Palms to the southeast end of the Indio Hills. Similar to the Banning fault, the Mission Creek fault dams ground water and creates a high water table on the northeast side of the fault. The most prominent areas of vegetation along the fault are located at Two Bunch Palms and Thousand Palms Oasis. The water table is located within 5 meters (16 feet) of the surface at Two Bunch Palms (Proctor, 1958). Several other oases supporting palm trees and mesquite appear along the fault as small dots on the imagery. An alignment of cultivated plots, owing to the availability of near-surface ground water, can be seen along the north side of the fault between Two Bunch Palms and the northwest end of the Indio Hills.

To the southeast, the fault can be traced to Thousand Palms Oasis as an almost continuous alignment of linear valleys and ridges along the straight northeast edge of the Indio Hills. Within the Indio Hills, stream courses at three locations along the fault southeast of Thousand Palms Oasis appear to be deflected to the right an average of about 2 kilometers (1.2 miles). A straight break in slope appears along the middle stream offset, and a prominent linear valley with a parallel linear ridge uplifted along the

southwest side of the fault can be seen along the southeastern stream offset.

A linear valley along the Banning-Mission Creek fault appears on the Skylab image (Fig. 3) on the southwest edge of the Mecca Hills. The fault is covered for about 16 kilometers (10 miles) southeast of the Mecca Hills and reappears along the east shore of the Salton Sea. Two linear, dark areas are produced by juxtaposed formations of contrasting color along the fault. Upturned, red-brown continental sediments of Quaternary age occur on the northeast side, and younger lake sediments (Late Pleistocene or Recent), consisting of tan mudstone and tan fine-grained sandstone, occur on the southwest side.

The Banning-Mission Creek fault and uplifted and deformed Quaternary sediments are not in evidence on Skylab imagery southeast of these exposures. Thus, our interpretation of Skylab imagery is in accord with previous surface mapping and geophysical studies that suggest the San Andreas fault terminates, possibly at a spreading center, near the southeast end of the Salton Sea.

Southeastern Imperial Valley and Sonora, Mexico

Faults along the trend of the San Andreas southeast of the suggested spreading center would be comparatively inactive under the hypothesis that the San Andreas fault is a transform fault. However, significant vertical separation on the top of basement rocks could occur as a result of isostatic adjustment of crustal blocks of different thicknesses. East of the Salton Trough, deposits similar or correlative to the Imperial Formation (Pliocene) are exposed at an altitude of about 320 meters (1050 feet). Near the center of Imperial Valley, these deposits were not penetrated in a well bottoming at a depth of 4097 meters (13,443 feet) (Dutcher et al, 1972). The required vertical offset could be explained by a fault interpreted from geophysical surveys near the eastern margin of the Sand Hills (Kovach et al, 1962). The Sand Hills fault has been aligned with the Algadones fault southeast of Yuma, Arizona (Mattick et al, 1973). However, the Algadones fault cannot delineate the eastern margin of the Salton Trough in Sonora, Mexico, because a southeastern extension would lie east of exposures of basement rocks of possible Precambrian age in Sierra del Rosario (R. Merriam, personal communication).

Gravity and aeromagnetic data suggest 3 kilometers (2 miles) vertical separation at the top of basement rocks along a fault between sediments of the Salton Trough and basement rock exposed to the northeast in Sierra del Rosario (Sumner, 1972). Between the Salton Sea and Gulf of California, shifting sands and river flood plain deposits obscure any direct surface indications of faulting along the northeast edge of the Salton Trough. However, physiographic features appearing on Skylab imagery may be indicative of faulting along this trend. A prominent dark spot appears on the Skylab image (Fig. 4) on the approximate surface trace of the fault identified by Sumner. The dark spot is a lake (R. Merriam, personal communication) which, in this arid region, could be due to impoundage of ground water on the northeast side of a fault.

To the northwest, a remarkably straight tonal difference is located near the southwestern edge of the Sand Hills. The slightly darker tone on the northeast side is the result of denser vegetation. The depth to the water table is 35 to 45 feet (10 to 14 meters) in six wells along the edge of the Sand Hills (Loeltz et al, 1975). There is no evidence that the water table is displaced along the tonal change, but well control is poor in this area (J. H. Robison, personal communication, 1975). Vegetation consists of shallow-rooted bushes, so it is doubtful that the vegetation change could be due to blockage of ground water. Loeltz et al (1975) have suggested that the dune sand may have been supplied by beaches along a fault-controlled shoreline at the southwest edge of the dune field. The straight vegetation break may be the result of soil differences along the fault-controlled shoreline. A fault is also suspected on the basis of a well drilled on the southwest margin of the dune field (S. L. Werner, personal communication). The well was drilled on a geothermal anomaly by the California Department of Water Resources, and silicifed recent basin deposits were encountered (Werner and Olson, 1970).

Approximately half-way along the western edge of the Sand Hills, the dune field overlaps the line of vegetation and surficial evidence of faulting is obscured by cultivated fields and leakage along the Coachella Branch of the All American Canal. The overview provided by the Skylab images aided in the interpretation of this possible fault in the San Andreas set by showing the regional alignment of fault indicators at an appropriate scale.

The San Jacinto fault zone extends from near the San Andreas fault in the San Gabriel Mountains southeast 500 kilometers (300 miles) to the Gulf of California. In contrast to the continuous trace of the San Andreas fault, the continuity of any one fault trace cannot be proven over the length of the San Jacinto fault zone. Maps prepared by Dibblee (1954), Sharp (1967, 1972), Bartholomew (1970) and others, show different locations, extensions, and names for some of the principal faults within a zone of subparallel and branching faults up to 20 kilometers (12 miles) wide. A microearthquake study of the San Jacinto fault zone in San Jacinto Valley by Cheatum and Combs (1973) also indicates a complex fault pattern in a zone 20 kilometers (12 miles) wide.

The San Jacinto fault zone is characterized by high seismic activity; thirteen large earthquakes have occurred along the fault zone north of the Mexican border since 1890 (Lamar, Merifield, and Proctor, 1973). Surface faulting for a distance of about 31 kilometers (19 miles) with displacements of up to 38 centimeters (15 inches) occurred on the Coyote Creek fault during the 1968 Borrego Mountain earthquake (Clark, 1972). Surface rupture during an earthquake was also observed on the Imperial fault in 1940 and may have occurred in 1934 along faults in the San Jacinto fault zone in the Colorado River Delta. Sharp (1972) has compiled a map showing recently active breaks along the San Jacinto fault zone. According to Sharp (1967), fresh scarps and offset stream channels along the San Jacinto fault north of Anza indicate 730 meters (2400 feet) of recent right-lateral displacement, and the total right-slip on the San Jacinto fault zone amounts to about 24 kilometers (15 miles). This displacement was initiated during the Pliocene.

Two prominent linears appear on the Skylab images of the Colorado Delta area (Fig. 4). The western linear in recent deltaic deposits corresponds to the segment of the San Jacinto fault believed to have been active in 1934 (Allen et al, 1965). The eastern linear appears as a straight, sharp boundary between deltaic deposits on the west and dune sand on the east. Merriam (1965) states that the southeast end of this linear is a fault and describes extensions of the San Jacinto fault zone to the southeast in Sonora.

To the northwest in Mexicali Valley, the fault traces are obscured by cultivated fields. However, an inferred northwest extension of the western linear passes through the Cerro Prieto geothermal field (De Anda and Parides, 1964); the geothermal activity may be related to the fault zone. Northwest

of the geothermal area, faint differences in the tone of cultivated fields south of Mexicali can be seen across a line along the same trend (Figs. 2 and 4). No additional evidence concerning the origin of this linear was found during a field reconnaissance, but variations in the tone of the cultivated fields could be related to subtle differences in the soil. The lake sediments beneath Mexicali Valley are primarily interbedded silt and clay. Because of its better drainage qualities, silt is preferable for crops. Silt and clay juxtaposed along a fault could be reflected in different crops or land use. Because the subtle differences in tone along this possible strand within the San Jacinto fault zone occur over a wide area, the overview provided by the small-scale Skylab images was required for recognition of the strand.

The tonal difference cannot be traced northwest of a point 6 kilometers (4 miles) south of the international border, but a continuation of the same trend lines up with a fairly straight segment of the New River. Exposures along the New River north of the border were examined, but no evidence of faulting was observed. If a fault along this trend curves slightly and is situated west of the New River, it would be aligned with a queried fault in the San Jacinto fault zone shown by Jennings (1973).

The Coyote Creek fault is a major strand of the San Jacinto fault zone exposed in Coyote Canyon (Sharp, 1967). Southeast of exposures of the fault in bedrock, an abrupt linear contact between dark and light earth materials appears on Skylab imagery along the southwest edge of Coyote Mountain. This contact was field checked in a search for previously unrecognized evidence of faulting from the south end of Coyote Mountain to the north end of Borrego Valley. Bedrock and individual clasts in the alluvial fan deposits and talus on Coyote Mountain are stained dark brown to dark gray by desert varnish. In contrast, the younger windblown sand and alluvium in Borrego Valley are not varnished and are light gray to glistening white. Occasional floods and wind transport sediments from the outlet of Coyote Creek at the north end of Borrego Valley to the southeast along the edge of Coyote Mountain. The alluvium and windblown sand form a sharp, fairly straight contact with the older, varnished rocks primarily because the older, dark rocks in the canyons along the mountain front are shielded from the windblown sand and alluvium

moving down the valley. This has the effect of straightening irregularities in the contact between light and dark rocks.

The field investigation revealed no evidence of recent fault movement along the southwest side of Coyote Mountain; however, the general straightness of the mountain front may be in part the result of erosional retreat parallel to a straight fault scarp. In this well-mapped area, Skylab images provided no new information. In an unmapped area, the straight trace of the mountain front would have quickly directed attention to the possibility of a major fault along this trend.

EAST TRENDING FAULTS

The Transverse Ranges east of the San Andreas fault are characterized by a number of east trending faults. Left-slip of up to several kilometers is demonstrable on some of these faults, and displacements in older alluvium and terrace deposits attest to movements in Quaternary time (Hope, 1966). Segments of these faults appear as linears on the Skylab image (Figs. 2 and 3).

Blue Cut Fault

The Blue Cut fault is one of the major east trending faults of the eastern Transverse Ranges. Correlation of lithologic units across the fault indicates left-slip of up to 5-6 kilometers (3-4 miles) on the western portion of the fault since Jurassic (Hope, 1966, 1969b). The western end of the Blue Cut fault curves northward and merges with the northwest trending Dillon fault (Rogers, 1965). Discontinuous fault zone exposures and physiographic evidence suggest that the Blue Cut fault may continue east for 80 kilometers (50 miles) and terminate against a northwest trending fault near the western edge of the Coxcomb Mountains. Because the evidence of faulting is discontinuous and separated by considerable distances, the alignment of fault indicators cannot be appreciated on the ground, from low flying aircraft, or in RB-57 photos. A view eastward along the fault trend from a low-flying aircraft is shown in Fig. 8. The overview provided by small-scale Skylab imagery (Fig. 3) is ideal for recognizing the regional alignment of

the physiographic features described by Hope (1966) over the length of the fault.

Good exposures in the Blue Cut, an east-west canyon in the Little San Bernardino Mountains, reveal a near-vertical fault zone several hundred feet wide. East of the Blue Cut, the fault is buried beneath recent alluvium in Pleasant Valley, and reappears in El Dorado Canyon. The alignment of straight canyon segments eroded along the fault in the Blue Cut, the east end of Pleasant Valley, and along El Dorado Canyon, is quite apparent on the Skylab imagery (Fig. 3). A fault is located along the straight northeast edge of Pleasant Valley seen on Skylab imagery. The sharp linear at the east end of Pleasant Valley is formed by shadows on the north side of a ridge of fanglomerate uplifted on the south block of the Blue Cut fault (Hope, 1969b). The cluster of low hills in the western Pinto Basin outlines a north-northwest trending anticline in Tertiary or Quaternary sedimentary rocks. This anticline may be a drag fold formed as a result of left-slip along the proposed eastern extension of the Blue Cut fault beneath Pinto Basin (Hope, 1969b). At the east end of the Pinto Basin, a southern branch of the fault may be located at the gently curving, abrupt north edge of the Eagle Mountains which is prominent on Skylab imagery.

Porcupine Wash, Substation and Victory Pass Faults

The Porcupine Wash fault can be traced from Pinto Basin westward into the Little San Bernardino Mountains where the trace ramifies and apparently ends. Left-separation of 2.4 kilometers (1.5 miles) on a near-vertical contact between granodiorite and gneiss is demonstrable, and scarps in older alluvium indicate Quaternary activity (Hope, 1966). To the east, the Substation and Victory Pass faults have been mapped in the Eagle Mountains. The Substation fault appears to offset a swarm of rhyolite dikes about 3 kilometers (2 miles) in a left-lateral sense. Displacement on the Victory Pass fault has not been determined (Hope, 1966).

Physiographic indicators along these faults are prominent on Skylab imagery (Fig. 3). Two straight canyons are aligned along the trace of the Porcupine Wash fault. To the east a straight canyon and a fairly straight break in slope can be seen along the trace of the Substation fault. The regional alignment of the Porcupine Wash and Substation faults can be seen

on Skylab imagery. However, physiographic evidence of a connection between the faults cannot be found and we were unable to trace the Substation fault west of the termination shown on existing maps (Hope, 1966: Jennings, 1967).

A straight canyon and linear breaks in slope appear on Skylab imagery (Fig. 3) along the mapped trace of the Victory Pass fault. A western continuation of the fault is suggested by an east-west trending low-lying area within the Eagle Mountains. To the west, across the southern Pinto Basin, the photo linear is aligned with the east-west trending Pinkham Canyon. However, the fault could only be traced in the field about 1.5 kilometers (one mile) west of the termination shown by Jennings (1967) and 3 kilometers (2 miles) west of the termination shown by Hope (1966). The westernmost fault exposure is in a mine at the southwest corner of Sec. 36, T4S, R13E. At this location, the fault diverges from the photo linear and turns southwestward across Big Wash; the attitude of the fault is N68°W, 42°S parallel to foliation in metamorphic rocks. Three kilometers (2 miles) further west, almost continuous outcrops of metamorphic rock with a persistant north-south strike and east dip of foliation cross the photo linear; it is unlikely that a western continuation of the fault can pass through this location. Further west, alluvium in the low-lying area along the photo linear would obscure any evidence of faulting.

Orocopia Linear

Jennings (1967) shows the Orocopia linear as a concealed fault extending parallel to Interstate Highway 10 for about 32 kilometers (20 miles) within the broad east-northeast trending valley between the Eagle Mountains on the north and the Orocopia Mountains on the south. A fault along this physiographic feature was first suggested by Hill (1928). Biehler et al (1964) describe a gravity low which may be the result of a fault-bounded, sediment-filled trough along the linear. Individual rock units and fault trends do not match across the linear (Jennings, 1967) which also suggests the presence of a fault. The overview provided by Skylab imagery shows that the Orocopia linear is the most prominent east-west trending, low-lying topographic feature in the region; based on parallelism with known left-slip faults to the north displayed on Skylab imagery, it is suggested that the Orocopia linear may have formed as a result of erosion of shattered rocks along a left-slip fault zone.

OTHER FAULTS IN THE SALTON TROUGH AREA

The Palm Canyon fault appears as a distinct but irregular line for about 16 kilometers (10 miles) along the axis of Palm Canyon. The irregular trace probably results from erosion along a thrust surface which dips 20° to 40° east (R. V. Sharp, personal communication, 1973). Faulting involves pre-Cretaceous metamorphic rocks only, and there is no evidence of displacement of Quaternary alluvium at the mouth of the canyon.

The Indio fault appears as a prominent, straight topographic break for 10 kilometers (6 miles) in Quaternary sediments along the northeast edge of the Indio Hills (Fig. 5). Prominent scarps can be seen on the ground along the fault but are not apparent on the Skylab images.

The Hidden Hills fault can be seen as a 20 kilometer (12 mile) long, north-northwest trending, prominent, straight tonal change on Skylab imagery northeast of the Salton Sea. The origin of the tonal change is not known.

The Pattern of linears in the Sierra de los Cucapas (Fig. 2) seen from Skylab (Fig. 4) is similar to the fault pattern shown by Gastil et al (1971). The linears identified southeast of Yuma (Figs. 2 and 4) have locations similar to faults shown on an unpublished map prepared by Richard Merriam (scale: 1:250,000). Extensions of these linears shown on Fig. 2 southeast of the Fig. 4 Skylab image can be seen on the Skylab 2, Roll 4, Frame 136 image.

With the exception of the Palm Canyon fault, the faults identified on the Skylab images are high-angle faults with straight traces. Other low-angle thrust faults in the region are not recognizable because they have sinuous traces and lack diagnostic fault-controlled features which would allow their differentiation from geologic contacts of other origin.

CONCLUSIONS

The following indicators of faulting have been recognized in Skylab imagery of the Salton Trough area: (1) topographic features such as scarps, fault-line scarps, offset drainage, linear valleys and straight mountain fronts, (2) vegetation differences due to ground water blockage, and (3) lithologic differences across the fault producing contrasting tone, color or texture. High-angle, strike-slip faults are most apparent; low-angle

faults are generally not identifiable. The scale and perspective of the Skylab imagery is advantageous for observing the regional alignment of faults tens of kilometers in length. For example, surface evidences of the Blue Cut fault are discontinuous and separated by as much as 10 kilometers (6 miles). The alignment of exposed segments of the Blue Cut fault is readily apparent in Skylab photos but cannot be appreciated in larger scale photos. Utilizing this perspective, the following alignment of northwest trending linear features, which may reveal previously unrecognized segments of faults in the San Andreas set, were identified: (1) a tonal change across cultivated fields of the Mexicali Valley which is aligned with strands of the San Jacinto fault zone to the northwest and southeast, and (2) a straight break in vegetation and a lake in Sonora, Mexico, aligned with the active San Andreas fault zone to the northwest and a fault to the southeast previously inferred from geophysical evidence.

This same perspective, however, can prompt incorrect interpretation of disconnected linear features which may have unrelated origins. Possible extensions of the Substation and Victory Pass faults, suggested by study of Skylab photos, could not be identified on the ground. The overview provided by Skylab images can greatly increase the efficiency of regional fault investigations; analysis of Skylab images should precede the study of larger scale imagery and detailed field investigations.

ACKNOWLEDGEMENTS

The work reported herein was accomplished under NASA Contract NAS 2-7698. We wish to acknowledge valuable discussions with Mason Hill, Richard Merriam, Shawn Biehler, Robert V. Sharp, G. A. Davis, S. L. Werner and James H. Robison. Richard Merriam kindly provided us with unpublished maps of Sonora, Mexico, and Morlin Childers accompanied us on a reconnaissance of Mexicali and Imperial Valleys.

REFERENCES

Allen, C. R., 1957, San Andreas fault zone in San Gorgonio Pass, southern California: Geol. Soc. Amer. Bull., v. 69, p. 315-350.

Allen, C. R., St. Amand, P., Richter, C. F., and Nordquist, J. M., 1965, Relationship between seismicity and geologic structure in the southern California region: Seis. Soc. Amer. Bull, v. 55, p. 753-797.

Allen, C. R., Wyss, M., Brune, J. N., Grantz, A., and Wallace, R. E., 1972, Displacements on the Imperial, Superstition Hills, and San Andreas faults triggered by the Borrego Mountain earthquakes: in The Borrego Mountain earthquake of April 9, 1968; U.S. Geol. Survey Prof. Paper 787, p. 87-104.

Bartholomew, M. J., 1970, San Jacinto fault zone in the northern Imperial Valley, California: Geol. Soc. Amer. Bull., v. 81, p. 3161-3166.

Biehler, S., Kovach, R. L., and Allen, C. R., 1964, Geophysical framework of northern end of Gulf of California structural province: Amer. Assoc. Petrol. Geol., Mem. 3, p. 126-143.

Cheatum, C. and Combs, J., 1973, Microearthquake study of the San Jacinto Valley, Riverside County, California: in Proc. Conf. on Tectonic Problems of the San Andreas Fault System, Stanford Univ. Publ., Geol. Sci., v. XIII, p. 1-10.

Clark, M. M., 1972, Surface rupture along the Coyote Creek fault: U.S. Geol. Survey, Prof. Paper 787, p. 55-86.

Crowell, J. C., 1962, Displacement along the San Andreas Fault, California: Geol. Soc. Amer., Spec. Paper 71, 61 p.

De Anda, L. F. and Parides, E., 1964, La falla de San Jacinto y su influencia sobre la actividad geothermica en el valle de Mexicali, B.C., Mexico: Boletin de la Association Mexicana de Geologos Petroleros, v. XVI, No. 7-8, p. 179-181.

Dibblee, T. W., Jr., 1954, Geology of the Imperial Valley region, California: Calif. Div. Mines and Geol., Bull. 170, contr. 2, Chapter II, p. 21-28.

Dibblee, T. W., Jr., 1968, Displacements on the San Andreas fault system in the San Gabriel, San Bernardino, and San Jacinto Mountains, Southern California: in Proc. Conf. on Geologic Problems of San Andreas fault system; Stanford Univ. Publ. Geol. Sci., v. XI, p. 260-278.

Dutcher, L. C., Hardt, W. F. and Moyle, W. R., Jr., 1972, Preliminary appraisal of ground water in storage with references to geothermal resources in the Imperial Valley area, California: U.S. Geol. Survey Circular 649, 59 p.

Elders, W. A., Rex, R. W., Meidev, T., Robinson, P. T. and Biehler, S., 1972, Crustal spreading in southern California: Science, v. 178, p. 15-24.

Gastil, R. G., Phillips, R. P., and Allison, E. C., 1971, Reconnaissance Geologic Map of the State of Baja California: Geol. Soc. Amer. scale 1:250,000.

Hill, M. L., 1965, The San Andreas rift system, California and Mexico; in The world rift system: Canada Geol. Survey Paper 66-14.

Hill, R. T., 1928, Southern California geology and Los Angeles earthquakes: Southern California Academy of Sciences, 232 p.

Hope, R. A., 1966, Geology and structural setting of the eastern Transverse Ranges, southern California: Ph.D. thesis, Univ. Calif., Los Angeles, 201 p.

Hope, R. A., 1969a, Map showing recently active breaks along the San Andreas and related faults between Cajon Pass and Salton Sea, California: U.S. Geol. Survey, Open File Report.

Hope, R. A., 1969b, The Blue Cut fault, southeastern California, Geological Survey Research, 1969: U.S. Geol. Survey Prof. Paper 650-D, p. D116-D121.

Jennings, C. W., 1967, Geologic map of California, Salton Sea sheet: Calif. Div. Mines and Geol.

Jennings, C. W., 1973, State of California, preliminary fault and geologic map, scale 1:750,000: Calif. Div. Mines and Geol., Preliminary Report 13.

Kovach, R. L., Allen, C. R., and Press, F., 1962, Geophysical investigations in the Colorado Delta Region: J. Geophys. Res., v. 67, p. 2845-2871.

Lamar, D. L., Merifield, P. M., and Proctor, R. J., 1973, Earthquake recurrence intervals on major faults in southern California: in Geology, Seismicity and Environmental Impact, Assoc. Eng. Geol., Spec. Publ., p. 265-276.

Loeltz, O. J., Irelan, B., Robison, J. H. and Olmsted, F. H., 1975, Geohydrologic reconnaissance of the Imperial Valley, California: U.S. Geol. Survey Prof. Paper 486-K, 54 p.

Mattick, R. E., Olmstead, F. H., and Zohdy, A. A. R., 1973, Geophysical studies in the Yuma area, Arizona and California: U.S. Geol. Survey Prof. Paper 726-D, 36 p.

Merriam, R., 1965, San Jacinto fault in northwestern Sonora, Mexico: Geol. Soc. Amer., Bull., v. 76, p. 1051-1054.

Proctor, R. J., 1958, Geology of the Desert Hot Springs area, Little San Bernardino Mountains, California: M.A. thesis, Univ. Calif., Los Angeles.

Proctor, R. J., 1973, Map showing major earthquakes and recently active faults in the southern California region: in Geology, Seismicity and Environmental Impact, Assoc. Eng. Geol. Spec. Publ.

Rogers, T. H., 1965, Geologic map of California, Santa Ana Sheet: Calif. Div. Mines and Geol.

Sharp, R. V., 1967, San Jacinto fault zone in the Peninsular Ranges of southern California: Geol. Soc. Amer. Bull., v. 78, p. 705-730.

Sharp, R. V., 1972, Map showing recently active breaks along the San Jacinto fault zone between the San Bernardino area and Borrego Valley, California: U.S. Geol. Survey Map I-675.

Sumner, J. R., 1972, Tectonic significance of gravity and aeromagnetic investigations at the head of the Gulf of California: Geol. Soc. Amer. Bull., v. 83, p. 3103-3120.

Tyley, S. J., 1971, Analog model study of the ground water basin of the Upper Coachella Valley, California: Water Resources Division, U.S. Geol. Survey, open-file report, 89 p.

Wallace, R. E., 1970, Earthquake recurrence intervals on the San Andreas fault: Geol. Soc. Amer. Bull., v 81, p. 2875-2890.

Werner, S. L. and Olson, L. J., 1970, Geothermal wastes and the water resources of the Salton Sea area: Calif. Dept. of Water Resources Bull. No. 143-7, 123 p.